Figure S1. SW unfiltered radiance errors for CERES Aqua FM3 in clear-sky scenes over ocean with wind speeds of 2 m/s and 12 m/s as compared to that for simulations with wind speed of 5 m/s, which is used to construct the regression coefficients for clear-sky scenes over ocean.
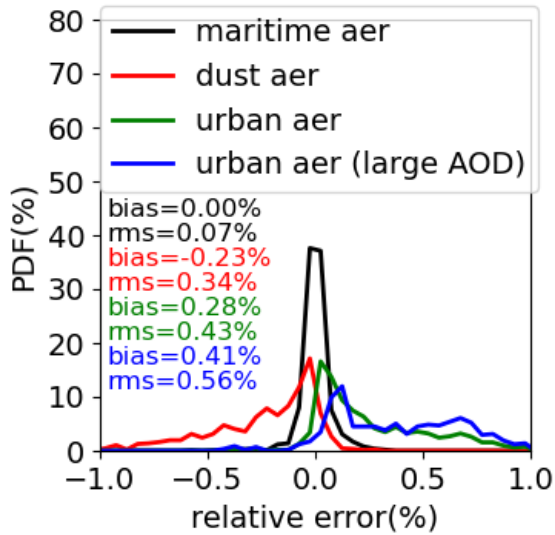
Figure S2. SW unfiltered radiance errors for CERES Aqua FM3 in clear-sky ocean scenes with dust, urban, and urban with large AOD aerosols as compared to that for simulations with maritime aerosol, which is used to construct the regression coefficients for clear-sky scenes over ocean.
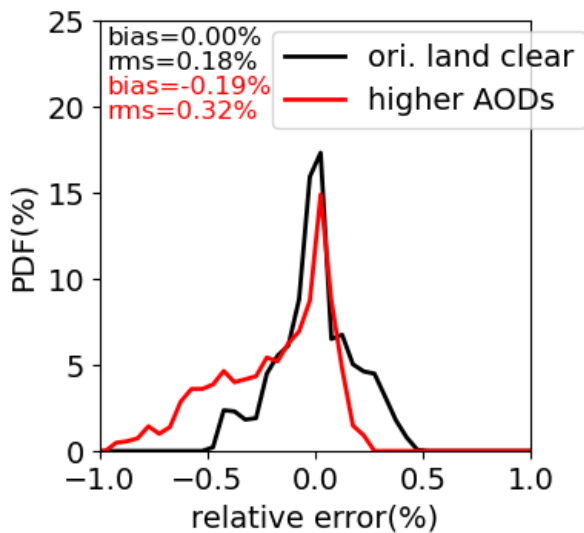
Figure S3. SW unfiltered radiance errors for CERES Aqua FM3 in clear-sky land scenes in July with large AODs (varying from 0.5 to 2.0 depending on surface types) as compared to errors in regression coefficients derived from clear-sky land scenes, where AODs used in simulations vary from 0.05 to 0.83 depending on surface type.
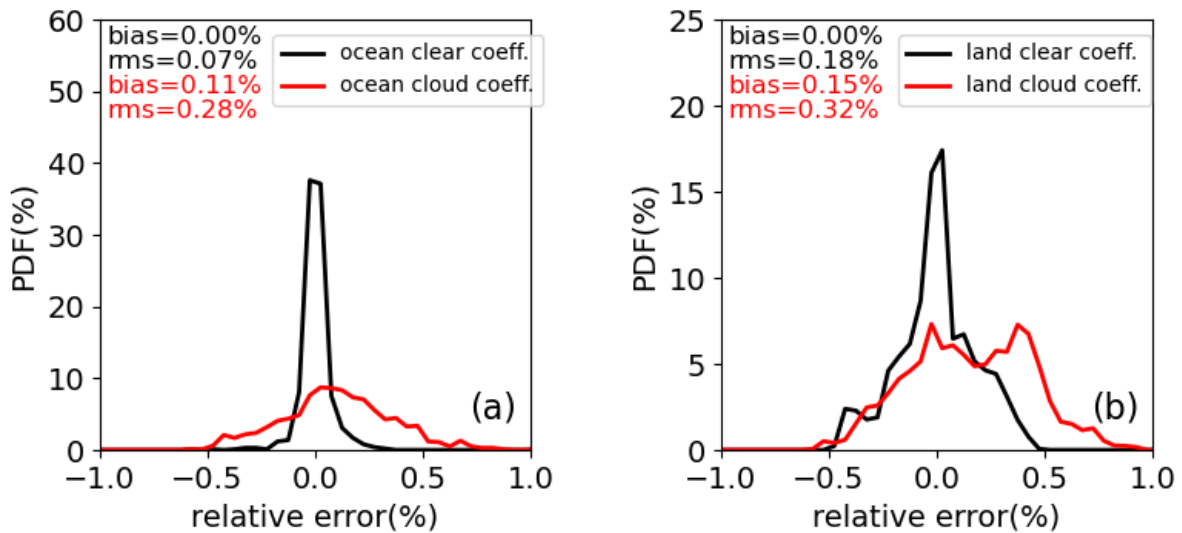
Figure S4. Comparison of SW unfiltered radiance errors for clear-sky scenes by using the regression coefficients derived from cloudy sky and clear-sky scenes over ocean (a) and land in July (b) for CERES Aqua FM3.
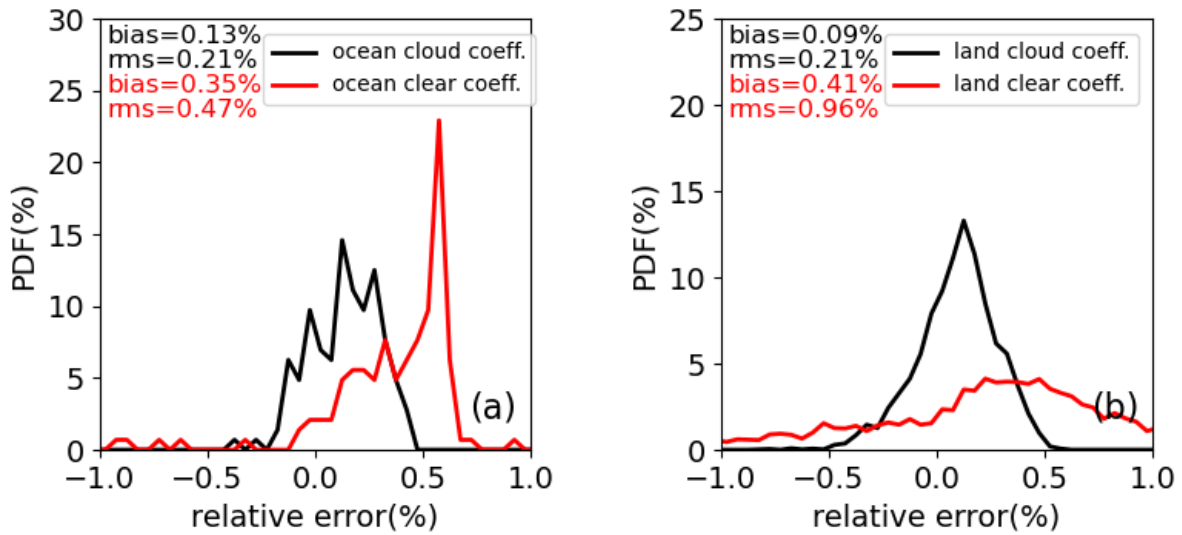
Figure S5. Comparison of SW unfiltered radiance errors for overcast scenes covered by cirrus (COD=2) by using the regression coefficients derived from clear-sky scenes and cloudy sky scenes over ocean (a) and land in July (b) for CERES Aqua FM3.
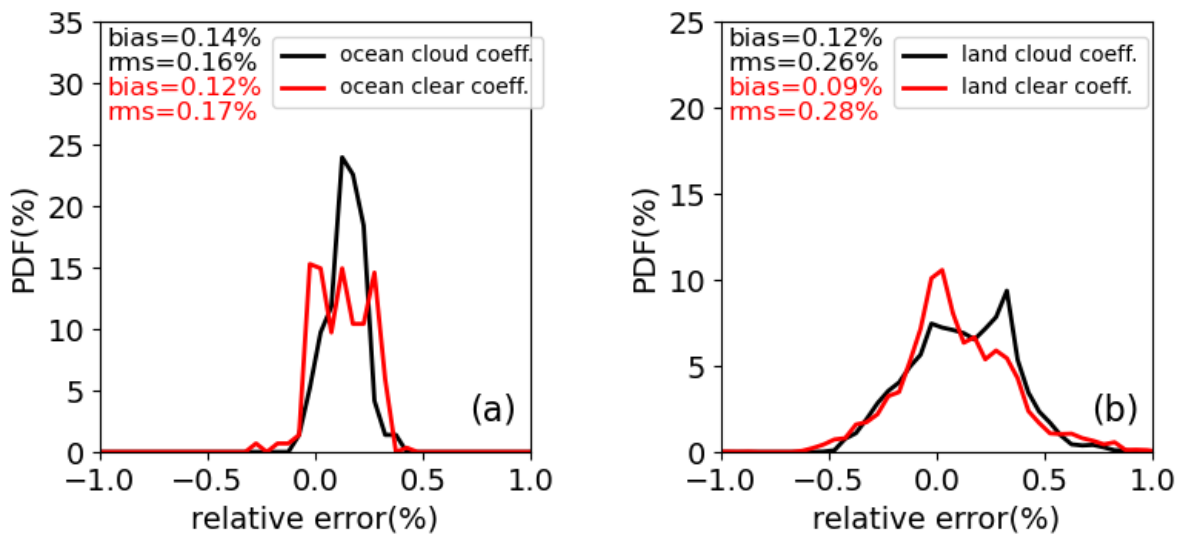
Figure S6. Comparison SW unfiltered radiance errors for CERES Aqua FM3 in broken cloudy-sky scenes (cirrus with COD=4 and stratus with COD=5.6 with a cloud fraction of 10%) by using the regression coefficients derived from cloudy sky scenes and clear-sky scenes over ocean (a) and land in July (b).
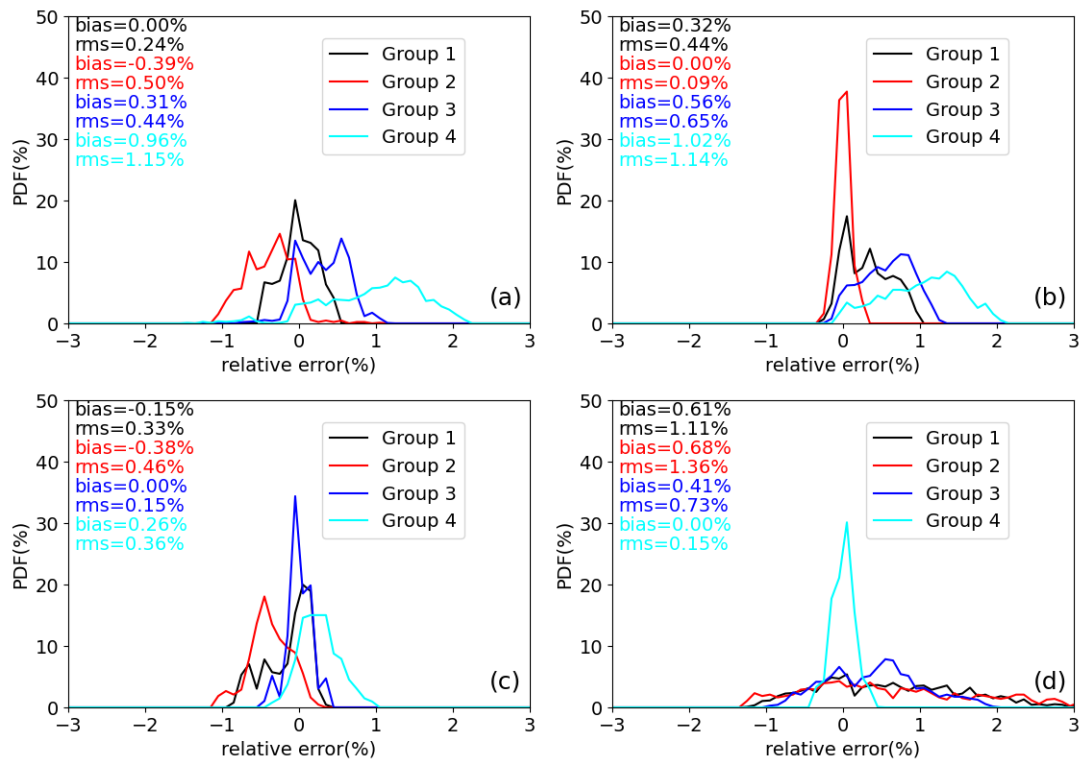
Figure S7. SW unfiltered radiance errors for land surface (a) Group 1, (b) Group 2, (c) Group 3, and (d) Group 4 by using regression coefficients derived from all 4 land surface types, respectively, for CERES Aqua FM3 in January. In January, Group 1 contains land surface IBGP types 01, 02, 04, 05, 08, 12 , and 14, Group 2 contains land IGBP surface types 03, 11, and 13, Group 3 contains land IGBP surface types 06, 07, 09, 10, and 18, and Group 4 contains land IGBP surface type 16.
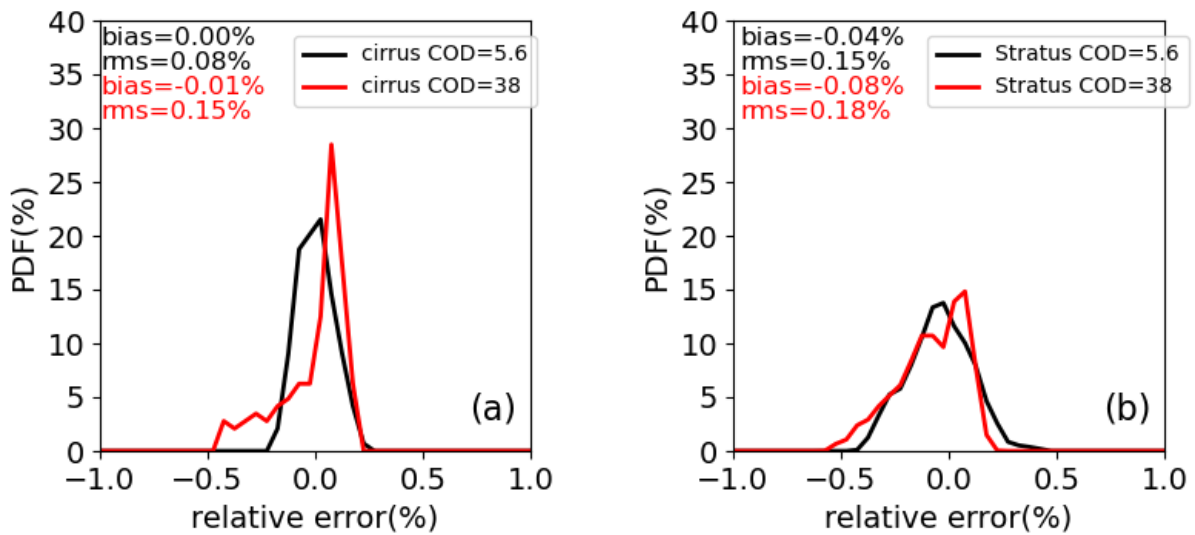
Figure S8. SW unfiltered radiance errors for CERES Aqua FM3 in cloudy sky scenes coved by stratus with COD of 38 as compared to that covered by stratus with COD of 5.6 by using regression coefficients derived from cloudy sky scenes over ocean (a) and land in July (b). Simulations with stratus of COD=5.6 are used to derive regression coefficients for cloudy sky scenes.
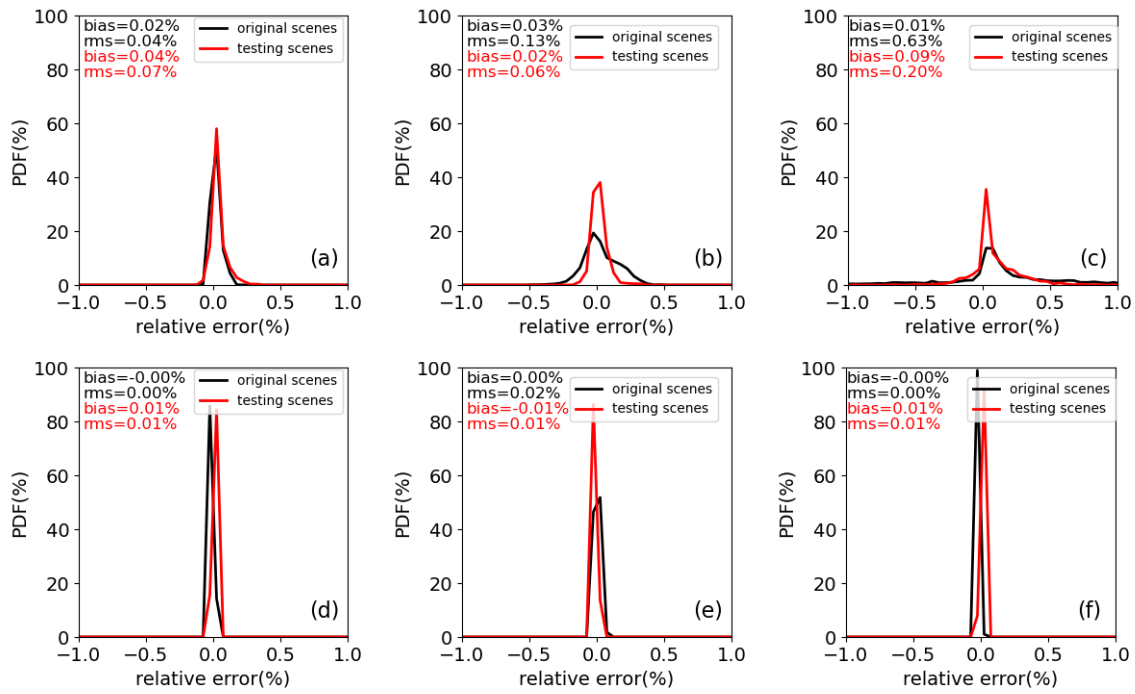
Figure S9. Daytime (a-c) and nighttime (d-f) LW unfiltered radiance errors for CERES Aqua FM3 in scenes with minimum and maximum climatological surface temperatures as compared to scenes with surface temperatures used in simulations to derive the regression coefficients for ocean (a and d), land (b and e) and snow (c and f). For ocean, the minimum temperature is set to 260K; for snow, the maximum temperature is set to 273K.
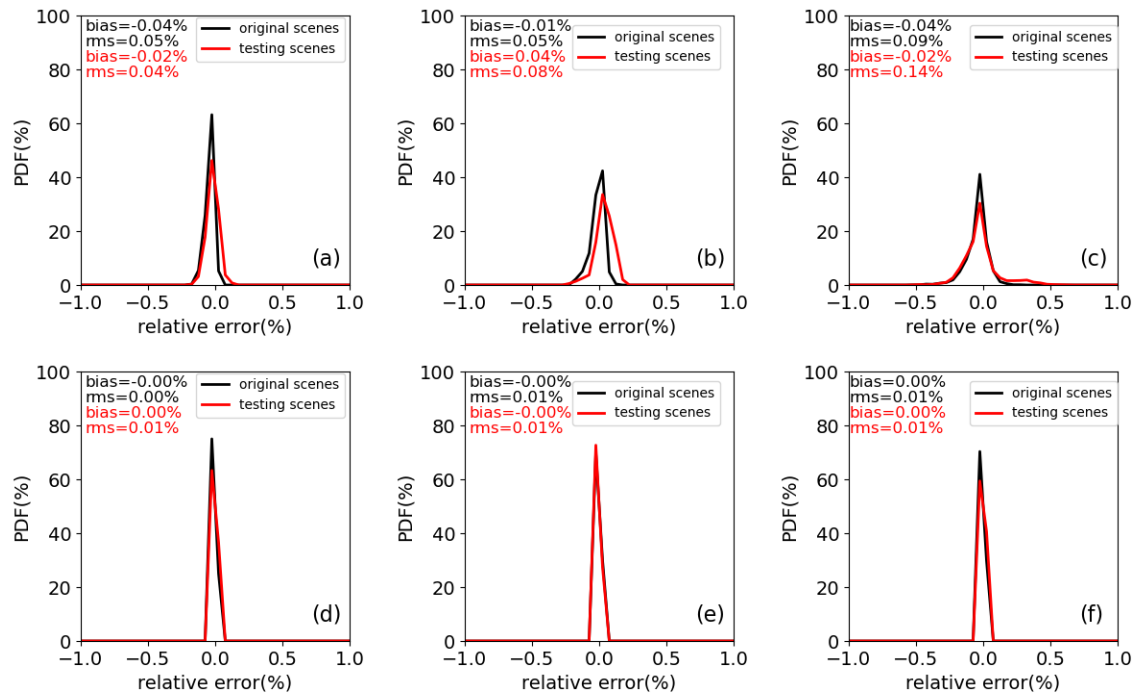
Figure S10. Daytime (a-c) and nighttime (d-f) LW unfiltered radiance errors for CERES Aqua FM3 in scenes with clouds places in different altitudes as compared to overcast scenes used in simulations to derive the regression coefficient database for cloudy sky over ocean (a and d), land (b and e) and snow (c and f).
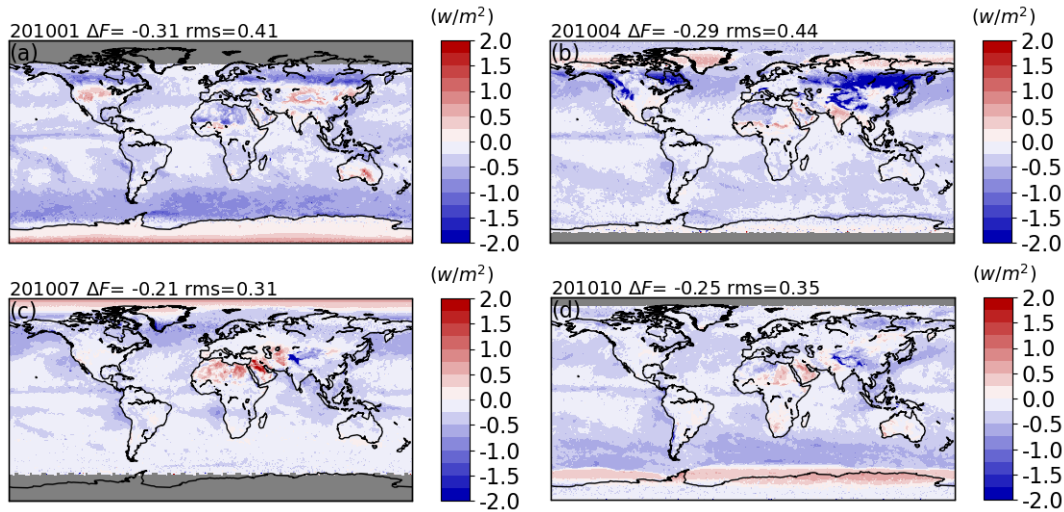
Figure S11. The differences between the SW instantaneous fluxes retrieved with unfiltered radiances based on the updated new CERES radiance unfiltering process and that based on the unfiltered radiances in the CERES Edition 4 product for CERES Terra FM1 instrument in April (a), July (b), October (c), and December (d).
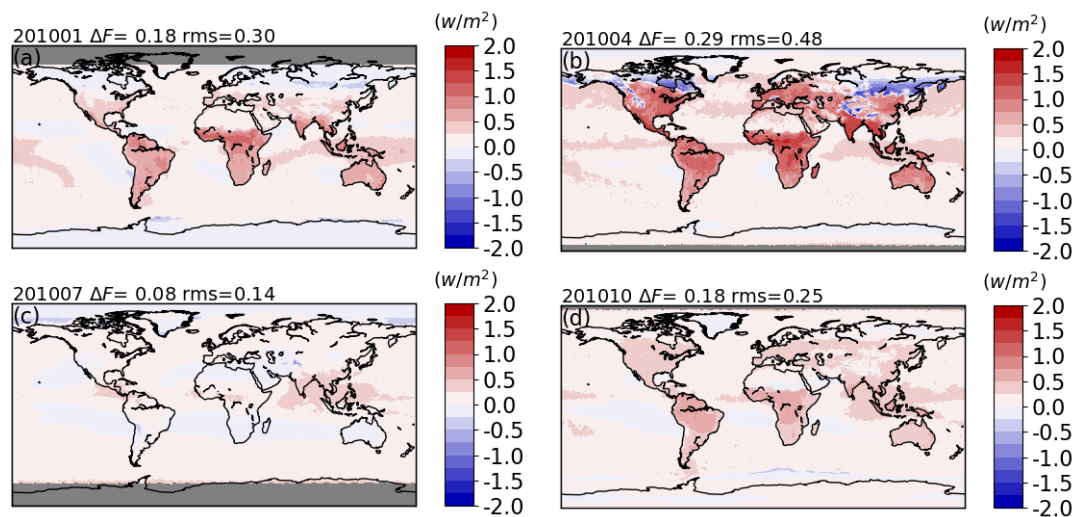
Figure S12. Same as Figure S11, but for daytime LW.
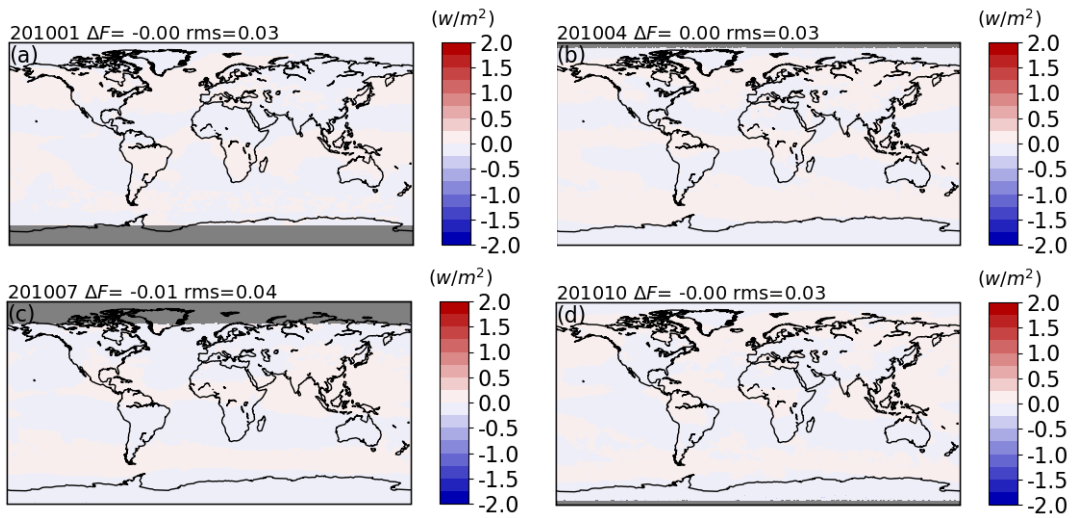
Figure S13. Same as Figure S11, but for nighttime LW.